Beam geometry calibration of SODARs without use of a mast

Bradley, SG and von Hünerbein, S

http://dx.doi.org/10.1175/JTECH-D-12-00112.1

Beam Geometry Calibration of SODARs Without Use of a Mast

Stuart Bradley[1]
Physics Department, University of Auckland, Auckland, New Zealand.

Sabine von Hünerbein
Acoustics Research Centre, University of Salford, Salford, UK.

[1] *Corresponding author address*: Stuart Bradley, Physics Department, University of Auckland, Private Bag 92019, Auckland, New Zealand.
E-mail: s.bradley@auckland.ac.nz

Abstract

A new method for calibration of SODAR wind speed measurements is described. The method makes no assumptions whatsoever about the SODAR operation and its hardware and software, other than the assumption that only one beam is transmitted at a time. Regardless of the complexity of the actual beam shape, the *effective* beam zenith angle is accurately estimated: this is the angle which must be used in estimations of velocity components. In a very simple experiment the effective beam zenith angle has been found to within around 0.2°, which is as good as is required in the most stringent SODAR calibration procedures. It has been found, even for such a short data run, that the estimated beam angle is very close to that calculated from the SODAR array geometry. The main limitation is the requirement for horizontally homogeneous flow, since the regression methods use both a tilted beam and a vertical beam. Note that this is also a fundamental limiting assumption in the normal *operation* of ground-based wind LIDARs and SODARs.

1. Introduction

SODARs transmit a short pulse in at least three upward directions. Scattering from atmospheric turbulent refractive index fluctuations results in a time series signal from each direction. Spectral analysis of time-gated segments of these time series gives a spectral peak whose frequency is a measure of the Doppler shift from the moving scatterers. Using at least three independent acoustic beams assures a system of at least three equations in the vector wind Cartesian components $\mathbf{V} = (u, v, w)$. Solving this set of equations then gives a wind profile with estimates at the centre of each height represented by the centre of each time gate (Bradley, 2007).

There is very little that can 'go wrong' with such a design. Nevertheless, large efforts have been expended on comparisons between mast-mounted anemometers and SODARs in such experiments as the Profiler Inter-comparison Experiment PIE (Bradley *et* al, 2005), directed toward remote-sensing becoming a viable replacement for mast instrumentation. The most important findings of PIE were that a SODAR gives similar variability in wind speeds to a cup anemometer, but there remain small *systematic* errors in wind speeds estimated by a SODAR. Such biases can be detected through SODAR-mast comparisons, but these are in general rather inconvenient. Therefore we consider a new method for doing *in-situ* field calibrations of wind measurements from a SODAR. This method has the huge advantages of not requiring comparison against some other 'standard', nor requiring any assumptions regarding SODAR geometry and operation.

The method is equally applicable to wind LIDARs. However, the emphasis on SODARs is warranted because it is difficult to test a full size SODAR system in an anechoic facility. Also, the acoustic beam from a SODAR has greater width than the optical beam from a LIDAR, and therefore the equivalent volume-averaged Doppler shift is likely to be less well known. This is rather difficult to estimate *a priori*, as opposed to the beam azimuth angle or the central pointing direction of a vertical beam, which are well determined by the SODAR antenna geometry.

2. SODAR wind measurement calibration

Traditional calibration

Monostatic SODARs use beams tilted from the vertical. The signal scattered back to the receiver in each tilted beam is Doppler-shifted according to the radial component V_r of wind velocity **V** in the beam direction. For a thin beam in direction $\mathbf{\Omega_0} = (\cos\phi_0 \sin\theta_0, \sin\phi_0 \sin\theta_0, \cos\theta_0)$ and wind velocity $\mathbf{V} = (u, v, w)$

$$V_r = \mathbf{V} \bullet \mathbf{\Omega_0} = u\cos\phi_0 \sin\theta_0 + v\sin\phi_0 \sin\theta_0 + w\cos\theta_0 . \quad (1)$$

At least 3 independent measurements are needed to solve for (u, v, w). We will concentrate on the typical 3-beam design. The system of equations

$$\mathbf{R} = \mathbf{BV}$$

is solved, where **R** is the 3x1 vector of measured radial velocity components, **B** is the 3x3 weighting matrix, and **V** is the 3x1 vector of unknown wind velocity components. The solution $\hat{\mathbf{V}} = \mathbf{B}^{-1}\mathbf{R}$ is used to form $\left(\hat{u}^2 + \hat{v}^2 + \hat{w}^2\right)^{1/2} = \left(\hat{\mathbf{V}} \bullet \hat{\mathbf{V}}\right)^{1/2}$ for comparison

with $\left(u^2+v^2+w^2\right)^{1/2}=\left(\mathbf{V}\bullet\mathbf{V}\right)^{1/2}$ measured by a mast-mounted anemometer. By this method a *single* calibration parameter

$$m=\left(\hat{\mathbf{V}}\bullet\hat{\mathbf{V}}\right)^{1/2}/\left(\mathbf{V}\bullet\mathbf{V}\right)^{1/2} \tag{2}$$

is obtained.

Consider the following simple example. A very narrow beam in the *x*-*z* plane, and with $w=0$ has $V_r=u\sin\theta_0$ so the wind estimate is $\hat{u}=V_r/\sin\theta_0$. If there is an uncertainty or an error $\Delta\theta$ in the tilt angle θ_0, then the uncertainty or error in estimated wind is $\Delta\hat{u}/\hat{u}=-\Delta\theta/\tan\theta_0$. For θ_0 =15°, each 1° error in beam pointing angle gives a 5% error in estimation of wind speed: Monostatic SODARs and LIDARs are ***highly sensitive*** to beam pointing.

Complete wind measurement calibration

The calibration parameter *m* in (2) contains combinations of elements from beam matrix **B**, which are functions of the three zenith angles and three azimuth angles for a three-beam system. In obtaining estimates of *u*, *v*, and *w*, these elements are *assumed* known in the SODAR processing software. Incorrect values of any of these elements will give a variation in *m*. This variation in *m* will also be *wind-direction dependent* as can be seen from the very simple case of a beam tilted an angle θ_0 in the *x*-*z* plane, another beam tilted θ_0 in the *y*-*z* plane, and the third beam vertical. Then

$$m^2=\left(\frac{\hat{V}}{V}\right)^2=\frac{\sin^2\theta_0}{\sin^2\hat{\theta}}+\frac{w\left(\cos\theta_0-\cos\hat{\theta}\right)\left[2(u+v)\sin\theta_0+w\left(2+\cos\theta_0+\cos\hat{\theta}\right)\right]}{\left(u^2+v^2+w^2\right)\sin^2\hat{\theta}}$$

where $\hat{\theta}$ is the tilt angle assumed by the software, and θ_0 is the actual tilt angle. This problem with traditional calibration methods has not been previously considered.

In practice however, the beam is not an angular delta-function and the weights in (1) are volume averages over the transmitted and received beams

$$V_r = u\overline{\cos\phi\sin\theta} + v\overline{\sin\phi\sin\theta} + w\overline{\cos\theta}\,. \tag{3}$$

The elements of **B** could be found in principle by measuring the beam angular intensity variations in an anechoic chamber, or perhaps in the field, but this effort would be large because of the need to capture beam details on a hemispherical surface in high angular resolution in 2D so that the proper volume averages can be calculated.

3. Tilt angle perturbation

Basic perturbation concept

Figure 1 shows the *x*-*z* plane for a SODAR having a beam at an initial effective tilt angle θ_1. If there is also a beam in the *y*-*z* plane tilted at an angle of θ_2 to the vertical, the equations corresponding to (1) are

$$V_{r1} = u\sin\theta_1 + w\cos\theta_1 \tag{4}$$

$$V_{r2} = v\sin\theta_2 + w\cos\theta_2 \tag{5}$$

$$V_{r3} = w\,. \tag{6}$$

Also shown is the entire SODAR rotated by an angle $\Delta\theta$ about the *y* axis. Now

$$V_{r1}^* = u\sin(\theta_1 + \Delta\theta) + w\cos(\theta_1 + \Delta\theta) \tag{7}$$

$$V_{r2}^* = u\sin(\Delta\theta)\cos\theta_2 + v\sin\theta_2 + w\cos(\Delta\theta)\cos\theta_2 \tag{8}$$

$$V_{r3}^* = u\sin(\Delta\theta) + w\cos(\Delta\theta)\,. \tag{9}$$

The $V_{r1}, V_{r3}, V_{r1}^*, V_{r3}^*$ quantities are measured, the tilt perturbation $\Delta\theta$ is known, and u, w, θ_1 and θ_2 are unknown. Equations (4) through (9) are non-linear in the unknowns, but can be solved by finding: w from (6); u from (9); $\sin\theta_1$ from (4) and (7); $\cos\theta_2$ from (5) and (8); and v from (5), giving

$$u = \frac{V_{r3}^* - V_{r3}\cos\Delta\theta}{\sin\Delta\theta}. \tag{10}$$

$$v = \frac{\left(V_{r2}V_{r3}^* - V_{r3}V_{r2}^*\right)\left(V_{r3}^* - V_{r3}\right)}{\sqrt{\left(V_{r3}^* - V_{r3}\right)^2 - \left(V_{r2}^* - V_{r2}\right)^2}} \tag{11}$$

$$w = V_{r3} \tag{12}$$

$$\sin\theta_1 = \frac{V_{r1}V_{r3}^* - V_{r1}^*V_{r3}}{V_{r3}^2 - 2V_{r3}V_{r3}^*\cos\Delta\theta + V_{r3}^{*2}}\sin\Delta\theta \tag{13}$$

$$\cos\theta_2 = \frac{V_{r2}^* - V_{r2}}{V_{r3}^* - V_{r3}}. \tag{14}$$

The effective tilt angle

As indicated in (3), components of **B** are volume averages. The volume averaging means that a normalized beam gain function $G(\Omega,\Omega_0)$ is averaged over solid angle $\boldsymbol{\Omega}$ around a pointing direction $\boldsymbol{\Omega_0}$ in each of the terms on the right of (1):

$$\begin{aligned} V_r &= \int_{\Omega} \boldsymbol{\Omega}\bullet\mathbf{V}G(\boldsymbol{\Omega},\boldsymbol{\Omega_0})d\Omega \\ &= \int_{\Omega} \left(u\cos\phi\sin\theta + v\sin\phi\sin\theta + w\cos\theta\right)G(\boldsymbol{\Omega},\boldsymbol{\Omega_0})d\Omega \end{aligned}$$

129
$$= u\int_{\Omega}\cos\phi\sin\theta G(\mathbf{\Omega},\mathbf{\Omega_0})d\Omega + v\int_{\Omega}\sin\phi\sin\theta G(\mathbf{\Omega},\mathbf{\Omega_0})d\Omega + w\int_{\Omega}\cos\theta G(\mathbf{\Omega},\mathbf{\Omega_0})d\Omega$$
$$= u\overline{\cos\phi\sin\theta} + v\overline{\sin\phi\sin\theta} + w\overline{\cos\theta}$$

130 (15)

131 where

132
$$\int_{\Omega} G(\mathbf{\Omega},\mathbf{\Omega_0})d\Omega = 1\,.$$

133 For a beam nominally in the *x*-*z* plane, there will be contributions from finite
134 azimuth angles ϕ. However, such beams are invariably symmetric in azimuth, so *G* is an
135 even function of ϕ and the integral

136
$$\int_{\Omega}\sin\phi\sin\theta G(\mathbf{\Omega},\mathbf{\Omega_0})d\Omega = 0\,.$$

137 This means that

138
$$V_r = u\overline{\cos\phi\sin\theta} + w\overline{\cos\theta} = u\sin\theta_1 + w\cos\theta_1\,.$$

139
140 The θ_1 appearing in (4) is therefore an *effective* beam tilt angle. If this is
141 perturbed by rotating the entire SODAR through $\Delta\theta$ about the *y* axis then, using an
142 angular coordinate system attached to the SODAR, $G(\mathbf{\Omega}, \mathbf{\Omega_0})$ remains unchanged but the
143 beam direction with respect to the wind **V** is now ($\cos\phi\sin[\theta+\Delta\theta]$, $\sin\phi\sin[\theta+\Delta\theta]$,
144 $\cos[\theta+\Delta\theta]$) . The first term on the right of (15) becomes

145

$$
\begin{aligned}
& u\int_{\Omega}\cos\phi\sin(\theta+\Delta\theta)G(\mathbf{\Omega},\mathbf{\Omega_0})d\Omega \\
& \quad = u\int_{\Omega}\cos\phi(\sin\theta\cos\Delta\theta+\cos\theta\sin\Delta\theta)G(\mathbf{\Omega},\mathbf{\Omega_0})d\Omega \\
& \quad = u\cos\Delta\theta\int_{\Omega}\cos\phi\sin\theta G(\mathbf{\Omega},\mathbf{\Omega_0})d\Omega + u\sin\Delta\theta\int_{\Omega}\cos\phi\cos\theta G(\mathbf{\Omega},\mathbf{\Omega_0})d\Omega \\
& \quad = u\cos\Delta\theta\overline{\cos\phi\sin\theta} + u\sin\Delta\theta\overline{\cos\phi\cos\theta} \\
& \quad = u\cos\Delta\theta\sin\theta_1 + u\sin\Delta\theta\cos\theta_1 \\
& \quad = u\sin(\theta_1+\Delta\theta)
\end{aligned}
\tag{146}
$$

This means that, although θ_1 is an effective zenith angle and not necessarily the same as the pointing zenith angle, we can validly do arithmetic such as $\sin(\theta_1+\Delta\theta)=\sin(\theta_1)\cos(\Delta\theta)+\sin(\Delta\theta)\cos(\theta_1)$ as in (4)-(14) above.

4. The effect of beam geometry on Doppler shift

In the above, the Doppler shift is contained in the elements of vector **R**. The weighting on each of the wind velocity components is volume-averaged, but this does not give any indication of the spread or shape of the Doppler spectrum from which, by detecting the peak position, the components of **R** are estimated.

The acoustic radar equation covers this in principle (Bradley, 2007). Including the dependence on frequency and on volume averaging, the spectral density of received power at the mono-static antenna equation becomes

$$
\frac{dP_R}{df} = c\tau\sigma_s\frac{e^{-2\alpha r}}{r^2}\int_{\Omega}\frac{dP_T}{df}G(\mathbf{\Omega})d\Omega\,. \tag{158}
$$

Here c is the speed of sound, τ is the pulse duration, σ_s is the scattering cross-section area per unit volume and per unit solid angle, α is the acoustic absorption, r is the range to the

scattering volume, dP_T/df is the power per unit frequency interval transmitted into solid angle $d\Omega$, and G is an angle-dependent sensitivity kernel. The atmospheric absorption and scattering parts have been taken outside of the scattering volume integral since they are only weakly frequency-dependent and it is assumed that they do not vary much within a typical scattering volume. Assuming a Gaussian-shaped transmitted pulse of spectral width σ_f, and that the Doppler spectrum is centered on f_D rather than transmitted frequency f_T,

$$\frac{dP_R}{df} \propto \int_{\Omega} \exp\left[-\frac{1}{2\sigma_f^2}(f - f_D)^2 \right] G(\mathbf{\Omega}) d\Omega .$$

Note that all commercial SODARs use an approximately Gaussian pulse shape.

For example, if the acoustic beam has sensitivity G at a zenith angle θ and azimuth angle ϕ, then the integral is

$$\int_0^{2\pi} \left\{ \int_{-\frac{\pi}{2}}^{\frac{\pi}{2}} \exp\left[-\frac{1}{2\sigma_f^2}\left[f - f_T\left(1 - 2\frac{u}{c}\sin\theta\cos\phi - 2\frac{v}{c}\sin\theta\sin\phi - 2\frac{w}{c}\cos\theta\right)\right]^2 \right] G \sin\theta d\theta \right\} d\phi . \quad (16)$$

The usual assumption is that the beam in the x-z plane is effectively an angular delta-function

$$G(\theta, \phi) = \cos\theta \delta(\theta - \theta_0)\delta(\phi).$$

Then the above integral becomes

$$\exp\left[-\frac{1}{2\sigma_f^2}\left[f - f_T\left(1 - 2\frac{u}{c}\sin\theta_0 - 2\frac{w}{c}\cos\theta_0\right)\right]^2 \right] \sin\theta_0 \cos\theta_0$$

so that the spectrum peaks at

$$f_x = f_T\left(1 - 2\frac{u}{c}\sin\theta_0 - 2\frac{w}{c}\cos\theta_0\right)$$

giving the expected radial component as in (1) with $\phi_0 = 0$. Similarly, it is usually assumed that the beam in the +*z* direction has the form $G(\theta,\phi) = \delta(\theta)\delta(\phi)$ so that that spectrum peaks at

$$f_z = f_T\left(1 - 2\frac{w}{c}\right).$$

More generally, it can be seen in (16) that there is a term in $\sin^2\phi$ so that there is a contribution from the traverse width of the beam in spite of *G* being even in ϕ. The influence of this term in *v* is to give a broader spectral peak but not to change the peak position substantially, so will be ignored in the following. Also, in general the effect of the $\sin\theta$ weighting on *u* is to bias the spectral peak to the equivalent of a larger effective θ_0. There is therefore a small change in the effective tilt angle, as expected. However, this does not change the methodology of the new calibration concept when the effective tilt angle is unknown anyway.

5. Error analysis

Writing σ_V for the uncertainty in wind speed *V*, (13) gives

$$\sigma_{\theta_1}^2 \approx \left(\frac{\tan\theta_1}{\tan\Delta\theta}\right)^2\left[\sigma_{\Delta\theta}^2 + \left(\frac{\sigma_V \sin\theta_1}{V}\right)^2\right].$$

To obtain a calibration accuracy of 1%, we need $\sigma_\theta \approx 0.2° \approx 4\text{x}10^{-3}$ radian. For $\theta_1 = \Delta\theta =$ 15°, and without any peak detection error, $\Delta\theta$ also needs to be measured to 0.2°. This is achievable with a linear actuator and a digital inclinometer. The accuracy of 10-minute averaged SODAR spectral peak estimation is typically $\sigma_V = 0.2$ m s^{-1}, so the term in σ_V is typically a factor 10 larger than the $\sigma_{\Delta\theta}$ term. What this means is that around 10 trials of

10-minute duration must be conducted in order to reduce the typical errors from peak detection to an acceptable level.

An alternative is to recast (13) in the form

$$Y = aX$$

where

$$Y = \frac{V_{r3}^2 - 2V_{r3}V_{r3}^* \cos\Delta\theta + V_{r3}^{*2}}{V_{r1}V_{r3}^* - V_{r1}^*V_{r3}}$$

and $X = \sin\Delta\theta$. The slope of the least-squares line through the origin is $a = 1/\sin\theta_1$.

A disadvantage of this method is that the radial velocity components may not be made available to the user by the SODAR manufacturer. They then need to be calculated based on the beam zenith angle assumed by the manufacturer, or the zenith angle calculated from the antenna parameters. An alternative, and much simpler procedure, is to assume that, in comparison with *u* and *v*, *w* is negligible, so

$$\frac{u^*}{u} - \cos\Delta\theta = \left(\frac{1}{\tan\theta_1}\right)\sin\Delta\theta$$

which means that θ_1 can be estimated from the slope of the straight-line fit through the origin, via

$$\tan\theta_1 = \frac{\sum_{n=1}^{N}(\sin\Delta\theta_n)^2}{\sum_{n=1}^{N}\left(\frac{u_n^*}{u_n} - \cos\Delta\theta_n\right)\sin\Delta\theta_n}.$$

In this case

$$\sigma_{\theta_1}^2 \approx \frac{2}{\sum_{n=1}^{N} \sin^2 \Delta\theta_n} \left(\frac{\tan^2 \theta_1}{1 + \tan^2 \theta_1} \right)^2 \left(\frac{\sigma_V}{V} \right)^2$$

where N measurements are taken at $\Delta\theta_n$, n=1,2,…,N. For $\theta_1 = 15°$, and $\sigma_V/V = 0.04$, three cycles of $\Delta\theta = 15°$ and 38° should give $\sigma_\theta < 0.2°$.

6. Field measurements

Field measurements on very flat land in western Denmark, have been completed on an ASC4000 SODAR mounted on a frame, which is then tilted using a 12V-powered linear actuator, as shown in Figure 2. The operator used a reversing switch to raise and lower the tilting platform in synchronism with the SODAR averaging time, so that one undisturbed averaging period was followed by an averaging period in which the actuator was moved. Tilt angle $\Delta\theta$ and 90-m wind speed vs time are shown in Fig. 3. The correlation between retrieved wind speed and tilt angle is strong. This is expected from (7), which shows that V_{r1}^* is essentially linear in $\Delta\theta$.

7. Data analysis

Wind vector components were recorded at 10 m height intervals from 30 m to 130 m. The beam zenith angle θ_1 was estimated from the least-squares slope of the line through the origin for both the $w = 0$ case and the full solution case. Variances of the Y values corresponding to each of the two tilt angles were used as least-squares weights, since it was expected that the radial wind variability would increase as the SODAR was tilted further. Figure 4 shows estimated θ_1 values at each height for the two cases. The lowest

height gives outlier values of angle, consistent with some clutter contamination from beam side-lobes when the beam is tilted. The estimated angle at the upper height (130 m) also appears to give an outlier, especially for the $w = 0$ case, consistent with the signal-to-noise ratio for SODAR signals decreasing rapidly above 120 m (see Fig. 5).

The expected value of θ_1 can be calculated from the phased-array geometry for this SODAR. An incremental phase shift of $\pi/2$ is used to change beam zenith angles. The beam maximum will therefore be at a zenith angle of $\theta_1 = \sin^{-1}(\lambda/4d)$ where λ is the wavelength and d is the array element spacing. In the case of this SODAR, the transmitted frequency was 4500 Hz, and the speakers have a diameter of 0.085 m but are used in diagonal rows of spacing $d = 0.085/2^{1/2} = 0.06$ m. Taking into account the mean air temperature at SODAR height during the experiment, $\theta_1 = 18.32°$. This compares with the estimated zenith angle from the two cases given in Table 1.

8. Conclusions

Since Doppler measurement is inherently calculable, the main source of systematic calibration errors for SODARs is uncertainty regarding the effective beam pointing angle.

A new method for beam geometry calibration of SODARs is described. The method makes no assumptions about the SODAR operation and its hardware and software, other than the assumption that only one beam is transmitted at a time, and that the flow is horizontally homogeneous. Regardless of the complexity of the actual beam shape, the *effective* beam tilt angle is accurately estimated: this is the angle which must be used in estimations of velocity components. In a very simple experiment the effective beam zenith angle has been found to within around 0.2°, which is as good as is required

in the most stringent SODAR calibration procedures. It has been found, even for such a short data run, that the estimated angle is very close to that calculated from the SODAR array geometry.

Atmospheric refraction effects are not significant here. For example, with a beam zenith angle of 45°, an adiabatic lapse rate, and a height range of 100 m, the change in propagation angle is only around 0.1°. The main limitation evident at this stage is the requirement for horizontally homogeneous flow, since the regression methods use both a tilted beam and a vertical beam. Note that this is also a fundamental limiting assumption in the normal *operation* of ground-based wind LIDARs and SODARs. However, since horizontal homogeneity of the flow is assumed, this method should only be applied over flat homogeneous terrain, and not when strong vertical gradients might be expected. The vertical gradient restriction is because there is also the assumption that the wind at a particular radial distance for the artificially tilted beam is the same as the wind at the same range without artificial tilting. For example, with the 40° artificial tilt applied here, this means that the wind at 100 m height should be similar to the wind at 80 m height. Given the extended vertical sampling volume of the SODAR, this assumption will not normally cause significant errors. Note that both SODARs and LIDARs are used with the assumption (generally not stated) that the sampling in the vertical, via ‘range gating’, is adequate to describe the vertical structure of the wind, and that spatial aliasing is not occurring.

There are a number of reasons why the method described above is of practical importance. These include the fact that there will be a bias in measured Doppler shift compared to that calculated from simple beam geometry because, for a beam symmetric

around the central tilted direction, the angles between wind vector and portions of the beam are not symmetrical about the central direction. Furthermore, there can be bias arising from clipping of the beam by acoustic baffles surrounding the instrument, and these effects are generally difficult to estimate or measure in other ways. Similarly, it is challenging to calculate with confidence the beam shape of a SODAR based on small parabolic dish reflectors, such as the AQ500. Even for a SODAR based on a phased array of transducers, the beam shape details depend on the relative gains of the transducer elements, which may not be known with confidence, especially after the SODAR has been deployed in the field for some time.

Acknowledgments.

The authors are grateful to support from Michael Courtney, Torben Mikkelsen, the Høvsøre staff at Riso/DTU, and to Christine Bradley for field observations.

References

Bradley S. G., 2007: Atmospheric Acoustic Remote Sensing. CRC Press/Taylor and Francis Group, 271pp.

Bradley S.G., I. Antoniou, S. von Hünerbein, D. Kindler, M. de Noord, and H. E. Jørgensen, 2005: SODAR calibration for wind energy applications. Manchester, UK, University of Salford. 69pp.

List of Figures

TABLE 1. Comparison between estimated beam zenith angles and the calculated zenith angle.

	Mean θ_1	$\sigma_{\text{mean }\theta}$	Estimated-calculated θ_1
Calculated θ_1	18.32°		
θ_1 estimated with $w = 0$	18.27°	0.23°	-0.05°
θ_1 estimated with $w \neq 0$	18.55°	0.54°	0.23°

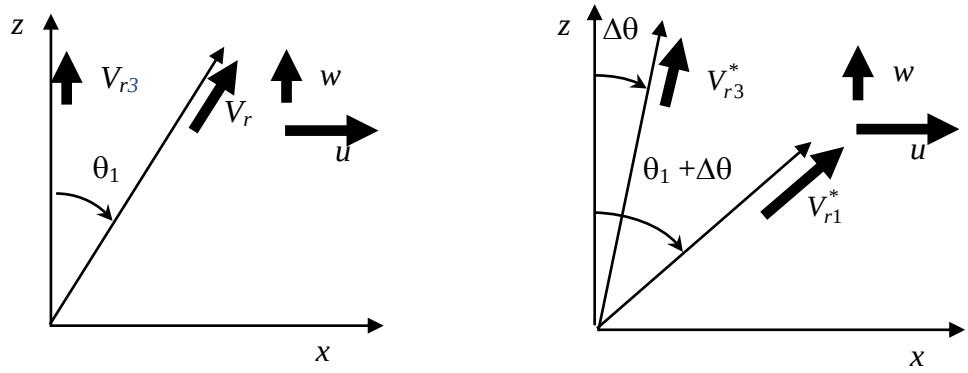

FIG. 1. The geometry of a SODAR beam tilted at an angle θ_1 (left diagram) and with the SODAR rotated by an angle $\Delta\theta$ about the y axis (right diagram). The wind velocity components in this plane are *u* and *w*, and the along-beam radial components for the two beams in this plane are V_{r1} and V_{r3}.

FIG. 2. The mounting frame and linear actuator, with digital level (left photograph) and measurements being taken (right photograph).

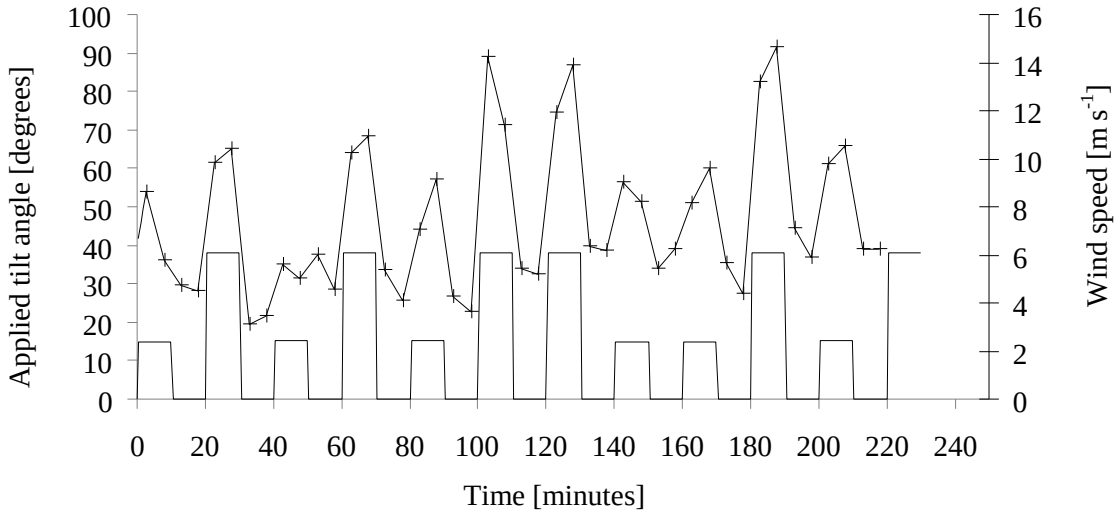

FIG. 3. Wind speed (crosses) and tilt angle (solid line) plotted versus time.

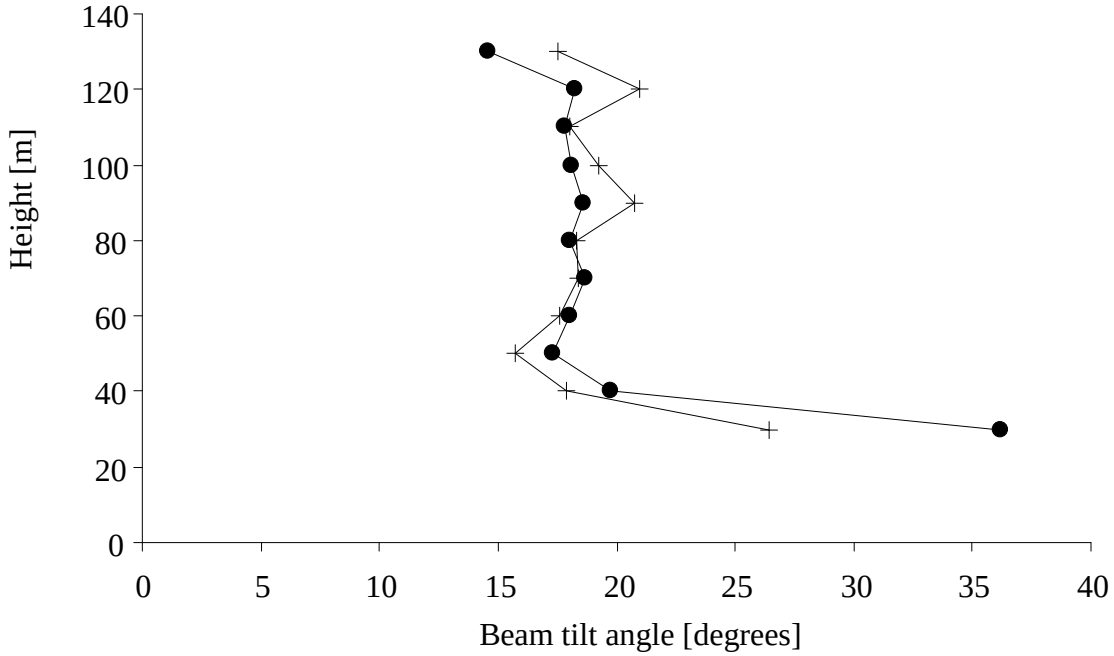

FIG. 4. Estimated beam zenith angles θ_1 from the w=0 case (filled circles) and the unconstrained w case (plus signs).

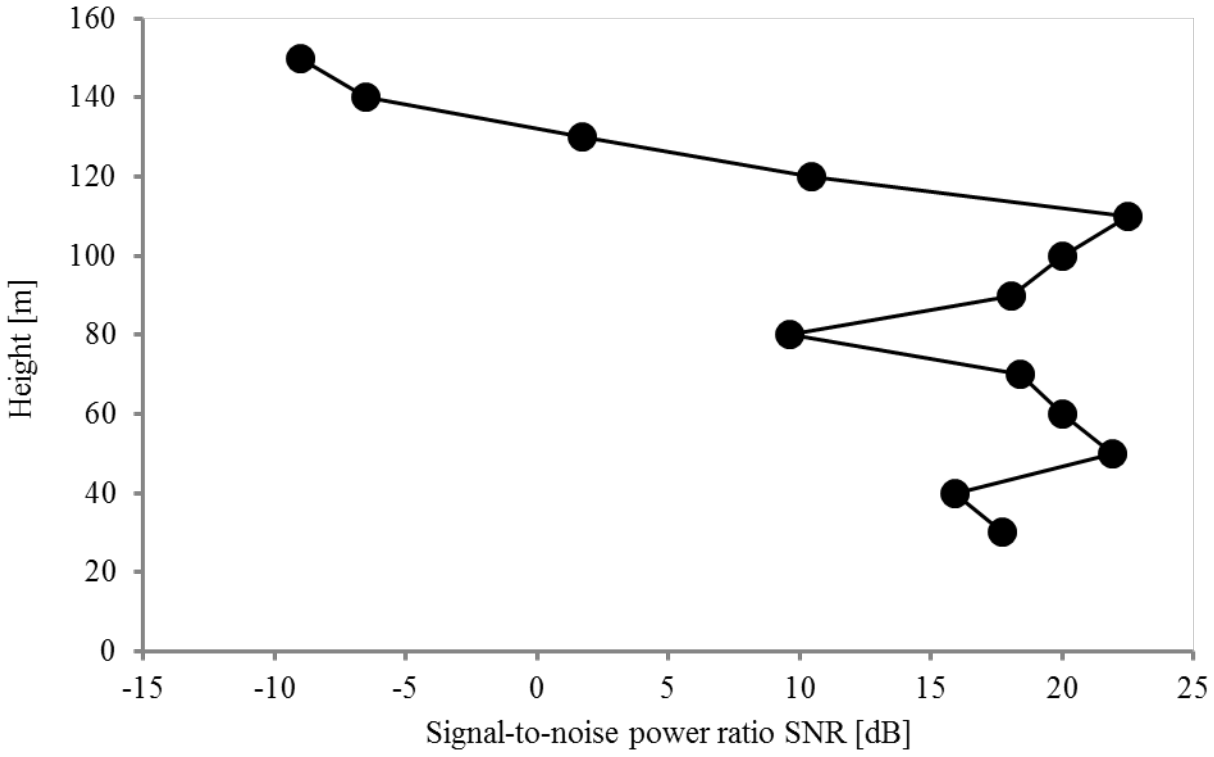

374

375

376 FIG. 5. The mean ratio of signal power to noise power (SNR) for the *w* beam, as a

377 function of height.

378